

## Neutron flow or collective degrees of freedom for near barrier heavy-ion fusion

S KAILAS and A NAVIN

Nuclear Physics Division, Bhabha Atomic Research Centre, Bombay 400 085, India

MS received 30 March 1993

**Abstract.** Various models have been proposed in order to understand the near barrier heavy-ion fusion data. Amongst others the coupled channel approach of Dasso and Landowne and the neutron flow picture of Stelson are two of the mechanisms which describe well a large body of near barrier fusion data. From an analysis of  $^{16}\text{O}$  induced fusion reaction around the barrier for various targets an attempt has been made to identify which out of the above two mechanisms is more appropriate to explain these data.

**Keywords.** Fusion reactions near Coulomb barrier;  $^{16}\text{O}$  projectile; targets with A values between 120 and 186.

**PACS No.** 25-70

### 1. Introduction

The study of heavy-ion fusion reactions near the Coulomb barrier continues to be of considerable interest [1]. Out of the many theoretical prescriptions proposed to describe the near barrier fusion cross-sections, the coupled channel approach [2, 3] and the neutron flow picture [4–6] are the most successful. The former is based on the fact that couplings of the incident channel to other non-elastic channels e.g. inelastic and transfer modify (both lower and raise) the barrier height and lead to an enhancement of the fusion cross-section near the 1-dimensional barrier. The Stelson model attributes the enhancement of the fusion cross-section to the onset of neutron flow due to the exchange of neutrons between the interacting nuclei (eventually leading to fusion) at a distance larger than the barrier radii. These two models also predict different barrier distributions.

Recently Vandenbosch [7] has made a comparison of these two models for the systems analyzed by Stelson and his collaborators and concluded that from the data analyzed one cannot choose between these models. The data used in that work were for different projectiles and targets. In the present work an attempt has been made to determine as to which out of the two mechanisms proposed for near barrier fusion is more appropriate, by choosing for an analysis, data for a single projectile  $^{16}\text{O}$ , interacting with several targets having mass numbers ranging from 120–186. Thus it is ensured that the effect of the projectile is a common factor in all the systems studied.

## 2. Models for fusion

### 2.1 The neutron flow model of Stelson

Stelson [4, 5, 6] suggested that near barrier fusion cross-section is dominated by neck formation initiated by neutron flow between the colliding nuclei at distances typically 1 to 2 fm larger than the mean barrier distance. He showed that if one assumed a flat distribution of barriers  $D(B)$ , symmetric about a mean barrier  $B$  and having a sharp lower cut-off at  $T$  (which is determined by the distance of approach at which the least bound neutrons may flow from one nucleus to the other), the usual expression for fusion cross-section (for energies greater than the barrier  $B$ )

$$\sigma_{\text{fus}}(E) = \pi R_b^2 \left( 1 - \frac{B}{E} \right), \quad (1)$$

becomes for near barrier energies

$$\sigma_{\text{fus}}(E) = \frac{\pi R_b^2}{4E} \frac{(E - T)^2}{4E(B - T)}, \quad (2)$$

where  $R_b$  is the barrier radius.

Assuming a neutron shell-model potential centered on each of the interacting nuclei he calculated the maximum value of the merged neutron potential  $V_n(\text{max})$  at a distance  $R$ , which is the distance at which the threshold barrier  $T$  is reached. (The mean barrier  $B$  is reached at a distance  $R_b$  in the total potential versus relative distance plot). According to Stelson, if the maximum of the merged neutron shell model potential  $V_n(\text{max})$  is deeper than the binding energy of the valence neutron  $S_{2n}/2$  of the two interacting nuclei the neutron flow is possible from the target to projectile and vice versa. As can be seen from figure 1, for both  $^{144}\text{Sm}$  and  $^{154}\text{Sm} + ^{16}\text{O}$  systems the neutron flow is possible only from the target to projectile. This point is further discussed in §3.3. From a systematic study of near barrier fusion data, he found a correlation between the  $T$  values and the average neutron separation energy  $S_n = S_{2n}/2$  (to take into account the odd-even effect in the neutron separation energy) and  $V_n(\text{max})$ . It is conceivable then that the extent of the barriers i.e.  $B-T$  values are also correlated with  $VSN = V_n(\text{max}) - S_{2n}/2$ .

### 2.2 Coupled channel model

It has been pointed out [2,3] that the coupling of the incident channel to other channels such as inelastic and transfer can modify the barriers. By calculating the transmission through the new barriers (with their appropriate weights) the fusion cross-section can be obtained. The change in height and the weights of these new barriers depend on the strength of the couplings ( $F_i(r)$ ) of the  $i$ th state coupled to the ground state and the  $Q$  value of that state. To simplify calculations they have made use of the constant coupling approximation i.e. the  $r$  dependence of  $F_i(r)$  is neglected and is replaced by its representative value  $F_0 = F(R_b)$ , where  $R_b$  is the barrier radius for a given system. The coupling strength for inelastic excitations to collective states is calculated from the deformation parameter  $\beta_{\lambda k}$  as [assuming

Coulomb and nuclear deformation parameters to be the same],

$$F_k(r) = \frac{\beta_{\lambda k}}{\sqrt{4\pi}} \left[ -R_k \frac{dV_n(r)}{dr} + \frac{3Z_1 Z_2 e^2}{(2\lambda + 1)} \frac{R_k^\lambda}{r^{\lambda+1}} \right], \quad (3)$$

where  $\lambda$  is the multi-polarity of the transition and  $k$  is the nuclei being excited (target or projectile).  $R_k$  is the radius of the nucleus ( $1.2A^{1/3}$  where  $A$  is the mass number) which is excited and  $V_n$  is the nuclear potential. The extraction of the radial dependence and strength of the form factor for the transfer channels is not so straightforward and involves the measurement of transfer angular distributions and their cross-sections for a particular system. There have been some attempts at obtaining the form factor for the transfer channels [8, 9]. However in the present work, only inelastic couplings have been considered. As the couplings ( $F$ ) lead to the barrier being lowered (or increased) it is expected in this model that the  $B$ - $T$  values will be related to  $F$ .

### 3. Correlation between B-T versus F and VSN

#### 3.1 Extraction of B, T and R values from the data

In the present work we have used the fusion data available for the following systems:  $^{16}\text{O} + ^{120}\text{Sn}$  [10],  $^{144}\text{Nd}$  [11],  $^{148, 150}\text{Nd}$  [12],  $^{144}\text{Sm}$  [13],  $^{148, 150, 152, 154}\text{Sm}$  [14],  $^{182, 184, 186}\text{W}$ ,  $^{176, 180}\text{Hf}$  [15],  $^{166}\text{Er}$ ,  $^{176}\text{Yb}$  [16]. The  $B$  and  $R_b$  values for the above system were obtained by fitting the fusion data at the above barrier energies using (1). The  $T$  values were determined by considering the data at near barrier energies (values lying between 10 and 150 mb) using (2).

#### 3.2 Determination of an effective $F'$

The quantity  $F$  (eq. (3)) has been determined for each system considering the inelastic excitation channels which include the low lying  $2^+$  and  $3^-$  states in both the target and the projectile, with no inter-couplings between them. The values of  $\beta_{\lambda k}$ ,  $\lambda$ ,  $Q$  were obtained from the literature [17, 18]. For each system the corresponding effective value of the coupling  $F'$  has been calculated as follows; At deep sub-barrier energies the extraction of an effective value of  $F'$  gets simplified [19]. We calculate the fusion cross-section with and without coupling and equate this ratio to  $e^{F'/\varepsilon}$  where  $\varepsilon$  is the barrier curvature. For each system the quantity  $F'$  has been determined using the code CCDEF [20, 21].

#### 3.3 Calculation of VSN

From the  $T$  values obtained as mentioned earlier the  $R_t$  values were determined using the approximate relation

$$R_t = \frac{Z_t Z_p e^2}{T}, \quad (4)$$

where  $Z_p, Z_t$  are charges of the projectile and the target respectively. For each target-projectile combination the maximum value ( $V_n(\text{max})$ ) of the sum of the shell model neutron potentials centered on the projectile and the target has been obtained by examining the potential energy at various positions along the internuclear axis

**Table 1.** Summary of near barrier fusion analysis projectile  $^{16}\text{O}$ . The error in  $B-T$  is given in the brackets.

Target	$R_b$ fm	$B$ MeV	$R_t$ fm	$T$ MeV	$B-T$ MeV	$F'$ MeV	$V_n(\text{max})$ MeV	$S_{2n}/2$ MeV	$VSN$ MeV
$^{120}\text{Sn}$	9.6	49.5	12.4	46.5	3.0(0.5)	0.67	9.1	7.8	1.3
$^{144}\text{Nd}$	10.0	56.7	12.6	54.7	2.0(0.4)	0.96	9.8	7.0	2.8
$^{148}\text{Nd}$	9.7	57.4	12.6	54.9	2.5(0.5)	1.35	10.5	6.3	4.2
$^{150}\text{Nd}$	9.4	57.3	12.8	54.1	3.2(0.4)	1.53	9.5	6.2	3.3
$^{144}\text{Sm}$	11.0	60.0	12.3	57.9	2.1(0.3)	0.90	12.0	9.5	2.5
$^{148}\text{Sm}$	10.3	59.3	12.8	55.8	3.5(0.5)	1.14	9.3	7.3	2.0
$^{150}\text{Sm}$	10.4	58.9	12.9	55.4	3.5(0.5)	1.28	8.8	7.0	1.8
$^{152}\text{Sm}$	9.4	57.8	13.1	54.5	3.3(0.4)	1.65	7.8	7.0	0.8
$^{154}\text{Sm}$	9.9	58.5	13.1	54.5	4.0(0.5)	1.75	7.9	6.9	1.0
$^{166}\text{Er}$	10.3	63.5	13.2	59.3	4.2(0.3)	1.93	8.3	7.6	0.7
$^{176}\text{Yb}$	12.6	64.1	13.4	60.2	3.9(0.5)	1.84	8.0	6.4	1.6
$^{176}\text{Hf}$	9.0	66.3	13.1	63.4	2.6(0.6)	1.82	9.9	7.5	2.4
$^{180}\text{Hf}$	9.4	65.9	13.2	63.0	2.9(0.5)	1.66	9.6	6.8	2.8
$^{182}\text{W}$	10.6	69.2	13.2	64.4	4.8(0.4)	1.62	9.3	7.4	1.9
$^{184}\text{W}$	10.7	68.8	13.3	64.2	4.6(0.4)	1.59	9.3	6.8	2.5
$^{186}\text{W}$	10.0	67.4	13.2	64.4	3.0(0.5)	1.47	10.0	6.5	3.5

keeping the interaction distance fixed at  $R_t$  following the procedure of Stelson [5]. The average separation energy  $S_{2n}/2$  values for the target have been obtained from the mass table [22]. The neutron flow initiated from the projectile  $^{16}\text{O}$  has not been considered here as the separation energy ( $S_{2n}/2$ ) is 14.4 MeV in this case and is much higher than the  $V_n(\text{max})$  values for all the targets considered here (see table 1). This is illustrated in figure 1, where the result of this type of calculation is shown for the  $^{16}\text{O} + ^{154}\text{Sm}$  and  $^{16}\text{O} + ^{144}\text{Sm}$  systems. It can be clearly seen that  $S_{2n}/2$  is larger than ( $V_n(\text{max})$ ) and hence it is not possible for neutron flow to take place from  $^{16}\text{O}$  to the target. Finally the quantity

$$VSN = V_n(\text{max}) - S_n \quad (5)$$

has been computed.

### 3.4 Comparison with the data

In table 1 we have collected the various quantities  $B$ ,  $R_b$ ,  $T$ ,  $R_t$  extracted along with the  $F'$ ,  $S_{2n}/2$ ,  $V_n(\text{max})$  and  $VSN$  values calculated in this work. It is interesting to compare the  $R_t$  values (obtained from the onset of fusion at the threshold barrier due to exchange of neutrons) with the  $D$  value obtained from heavy-ion single neutron transfer studies. The average value of  $R_t$  obtained from this work is

$$R_t = 1.65(A_t^{1/3} + A_p^{1/3}).$$

This value compares very well with the average value of  $D$  obtained from single neutron transfer studies which varies from 1.54 to 1.83 ( $A_t^{1/3} + A_p^{1/3}$ ) [23]. In figure 2a the  $B-T$  values have been plotted as a function of  $VSN$ . It is noticed that the  $B-T$

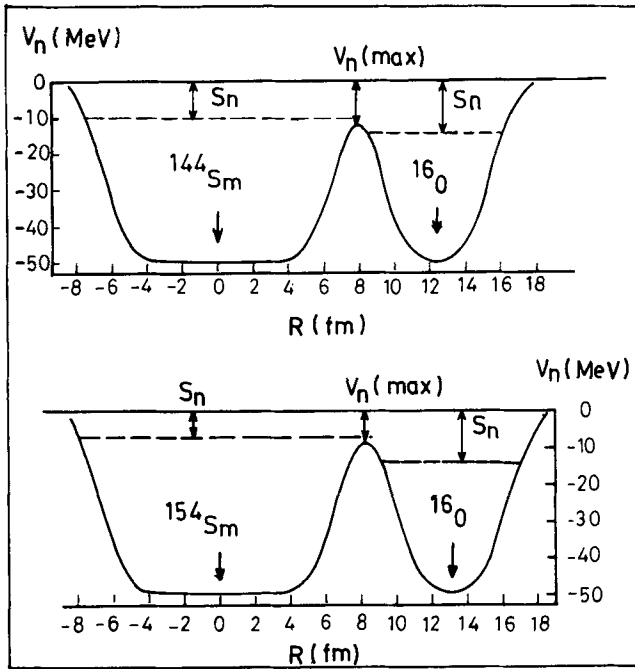


Figure 1. Merged neutron potentials at  $R$ , for  $^{144}\text{Sm}$  and  $^{154}\text{Sm} + ^{16}\text{O}$  systems. The  $V_n(\text{max})$  and the target/projectile  $S_n$  values are marked in the figure.

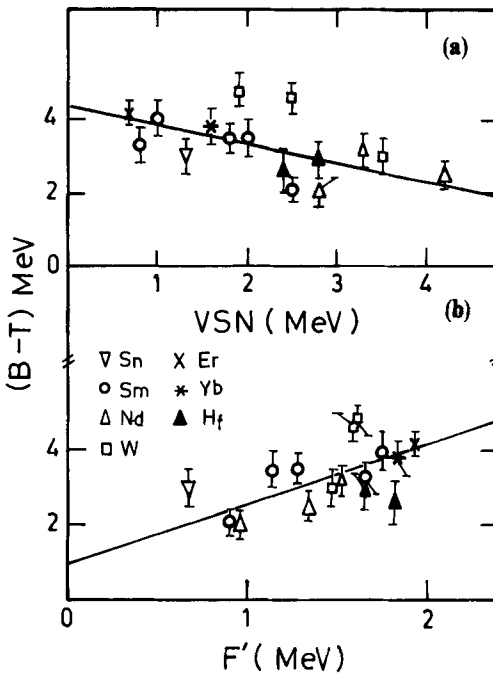
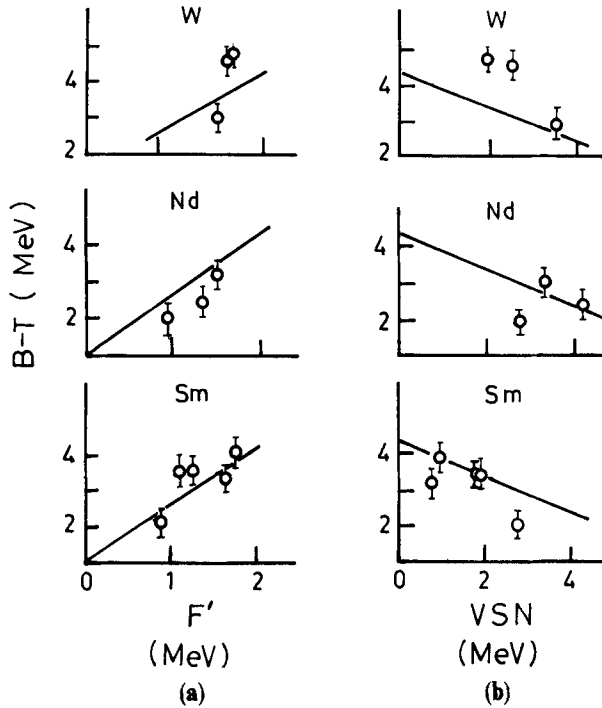


Figure 2. The  $B-T$  values determined for the various systems plotted against (a)  $V_{SN}$  and (b)  $F'$ . The straight lines represent the best linear fits to the data.



**Figure 3.** The  $B-T$  values obtained for Nd, Sm and W isotopes are plotted against  $F'$  and  $VSN$ . The straight lines are obtained using the global fit parameters of figure 2.

values on the average decreased with increase of  $VSN$  values but the correlation is not as striking as found between  $B-T$  and  $F'$ . Shown in figure 2b is the plot of  $B-T$  versus  $F'$ . From the figure one can observe a good correlation between the two quantities, an increasing value of  $B-T$  with increasing  $F'$ . Assuming a linear relationship between  $F'$  and  $B-T$  a fit to the data was made. A straight line adequately describes the data. A similar fit is made for the  $VSN$  versus  $B-T$  data. The  $\chi^2$  per degree of freedom for the latter fit was 30% worse than that obtained for the former one. In order to bring out the sensitivity of the models to the data, we have shown in figure 3 the  $B-T$  values for a range of isotopes for a given  $Z$  and compared them with  $F'$  and  $VSN$  estimates. The straight lines in this figure are obtained using the parameters determined in the earlier global fit. In general, both the models describe the trend of  $B-T$  variation. However the coupled channel approach is superior in describing the ( $B-T$ ) data.

#### 4. Summary

In the present work, from an analysis of near barrier fusion data available for  $^{16}\text{O}$  interacting with several targets with mass numbers ranging from 120 to 186, it is found that the deduced  $B-T$  values are better correlated with the variable  $F'$  (related to collective degrees of freedom) than with  $VSN$  (related to the neutron flow picture). The present results are suggestive that for  $^{16}\text{O}$  as projectile interacting with various targets, the collective degrees of freedom are more important than the neutron flow in influencing the near barrier fusion phenomenon. It will be interesting to make this kind of comparison for other projectiles as well.

## Acknowledgement

The authors thank Prof. R Vandenbosch for his interest in this work and helpful comments.

## References

- [1] C Signorini, S Skorka, P Spolaore and A Vitturi, (eds) *Proc. Int. Symp. on heavy ion interactions around the Coulomb barrier, Legnaro (Italy)* (1988)
- [2] C H Dasso, S Landowne and A Winther, *Nucl. Phys.* **A407**, 221 (1983)
- [3] R A Broglia, C H Dasso, S Landowne and G Pollarolo, *Phys. Lett.* **B133**, 34 (1983)
- [4] P H Stelson, in *Int. Symp. on heavy-ion reaction dynamics in tandem energy region*, Hitachi (Japan) August 1-3 (1988)
- [5] P H Stelson, *Phys. Lett.* **B205**, 190 (1988)
- [6] P H Stelson, H J Kim, M Beckerman, D Shapira and R L Robinson, *Phys. Rev.* **C41**, 1584 (1990)
- [7] R Vandenbosch, *Proc. eighth winter workshop on nuclear dynamics*, Jacksonhole Wyoming, USA Edited by W Bauer and B Back (World Scientific, USA) (1992)
- [8] L Corradi, S J Skorka, U Lenz, K E G Lobner, P R Pascholati, U Quade, K Rudolph, W Schomburg, M Steinmayer, H G Thies, G Montagnoli, D R Napoli, A M Steffanini, S Beghini, F Scarlassara, C Signorini and F Soramel, *Z. Phys.* **A334**, 55 (1990)
- [9] C H Dasso and G Pollarolo, *Phys. Lett.* **B155**, 223 (1985)
- [10] P Jacobs, Z Fraunkel, G Mamane and I Tserruya, *Phys. Lett.* **B175**, 271 (1986)
- [11] M di Tada (Private Communication 1992)
- [12] R Broda, M Ishihara, B Herskind, H Oeschler, S Ogaze and H Ryde, *Nucl. Phys.* **A248**, 357 (1975)
- [13] D Di Gregario, J O Fernandez Niello, A J Pacheco, D Abriola, S Gil, A O Macchivelli, J E Testoni, P R Pascholati, V R Vanin, Neto R Liguori, N Calin Filho, M M Coimbra, P R Silveira Gomes and R G Stokstad, *Phys. Lett.* **B176**, 322 (1986)
- [14] R G Stokstad, Y Eisen, S Kaplanis, D Pelte, U Smilansky and I Tserruya, *Phys. Rev.* **C21**, 2427 (1980)
- [15] J R Leigh, J J M Bokhorst, D J Hinde and J O Newton, *J. Phys.* **G14**, L55 (1988)
- [16] J Fernandez Niello, M di Tada, A O Macchivelli, A J Pacheco, D Abriola, M Elgue, A Etchegoyen, M C Etchegoyen, S Gil and J E Testoni, *Phys. Rev.* **C43**, 2303 (1991)
- [17] S Raman, C H Malarkey, W T Milner, C W Nestor Jr and P H Stelson, *At. Nucl. Data Tables.* **36**, 1 (1987)
- [18] R H Spear, *At. Nucl. Data Tables* **42**, 55 (1988)
- [19] S Landowne and S C Pieper, *Phys. Rev.* **C29**, 1352 (1984)
- [20] C H Dasso and S Landowne, *Comput. Phys. Commun.* **46**, 187 (1987)
- [21] J Fernández Niello, C H Dasso and S Landowne, *Comput. Phys. Commun.* **54**, 409 (1989)
- [22] A H Wapstra and R Hoekstra, *At. Data and Nucl. Data Tables* **39**, 281 (1988)
- [23] W Frahn and R H Venter, *Nucl. Phys.* **59**, 651 (1964)